

A Mathematical Model of Fractone-Controlled Morphogenesis

M. Chyba¹, F. Mercier², A. Tamura-Sato¹ and R. Zou^{1,3}

Abstract—It has been hypothesized that the generation of new neural cells (neurogenesis) resulting from stem and progenitor cell proliferation and differentiation in the developing and adult brain is guided by the extracellular matrix. The extracellular matrix of the neurogenic niches comprises specialized structures termed fractones, which are scattered in between stem/progenitor cells. Growing evidence indicates that fractones of the adult brain bind and activate growth factors at the surface of stem/progenitor cells to influence their proliferation. It has been shown that neuroepithelial cell proliferation is also associated with fractones during early brain development, although the functional links between fractones and neuroepithelial cells have not been elucidated. We present a mathematical model that considers the role of fractones as captors and activators of growth factors that influence the rate of proliferation and the location of the newly generated neuroepithelial cells in the forming brain. This model allows for the dynamic placement and removal of fractones into the evolving cell mass, giving us control over its developing shape. Using this model, we simulate early brain morphogenesis, focusing on the formation of the lateral ventricle walls from the anterior portion of the neural tube.

I. INTRODUCTION

The control of cell proliferation is a fundamental aspect of morphogenesis. To generate a shape, cells must proliferate in a spatially and temporally controlled manner. In the developing brain of vertebrate animals, the first neuroepithelial cells, which will later generate neurons and glia, proliferate and initiate a groove, which then closes to form a tube on the dorsal aspect of the embryo. Soon after, while still growing in thickness, the tube generates vesicles and grows lateral extensions that initiate the formation of the lateral ventricles (Fig. 1). Simultaneously, the neural tube undergoes a series of flexures in its antero-posterior axis that separates the cavity of the tube and forms the other ventricles. Then neuroepithelial cells differentiate and proliferate in concert to generate neurons and glia which compose the emerging specialized brain sub-structures. How does controlled cell proliferation generate these morphological events? The key molecules that control cell proliferation are growth factors. Growth factors are molecules that diffuse in the biological cavities as well as in the intercellular space. They influence cell differentiation and act as chemotactic agents, influencing cell migration [8], [11], [15]. Adding to the complexity,

growth factors are variably produced among developing tissues and throughout development and post-natal/adult life.

How can growth factors organize cell proliferation in the developing brain to generate a well-defined structure like the lateral ventricles emerging from the neural tube? A level of control by the extracellular matrix (ECM) has been hypothesized [7], [12]. The ECM exists under different forms, including the interstitial matrix (along the cell surface), basement membranes (sheet-like structure that are interposed between cell layers) and fractones, a new form of specialized ECM still under characterization. Fractones appear as puncta after immunohistochemical labeling for its proteoglycan components and visualization by fluorescence microscopy [6], [9], [13] and figure 1. In the adult brain, fractones are located at the surface of stem cells and their immediate progeny, influencing the rate of cell proliferation [6]. A possible mechanism is that the heparan sulfate proteoglycans that compose fractones bind the diffusing growth factors, store and present them to specific cell-surface receptors to ultimately control cell proliferation and differentiation [6], [14]. In the developing brain, fractones also co-localize with proliferating cells. The location of fractones constantly changes during development and strongly suggests that their emergence in a given location of the developing brain prepares a morphological event. Here, we hypothesize that embryonic fractones control the rate, location and timing of cell proliferation in the developing neural tube and post-neurulation events such as the formation of the lateral ventricles.

To support this hypothesis, we have developed a mathematical model of the interaction of cells, fractones, and growth factors. The model allows for control over the distribution of fractones over time by placing them with some controlled probability in certain regions of the developing brain. The diffusion of the growth factor and its binding caused by the presence of fractones is described using an affine control system defined on a dynamic configuration space, see [4], [3], [5] for early approaches. Indeed, every time mitosis occurs, the dimension of the configuration space varies. We also model the deformation of a mass of cells when one cell undergoes mitosis. This deformation is determined by the location of the fractone relative to the cell.

We use this model to simulate the formation of the lateral ventricles from the neural tube. At this stage, our model is an approximation of the biological process and does not capture all of the real features of the biological process. The distributions of fractones that we use in our simulations are based off of observations made in the lab, however, the complexity of the interactions between fractones, neuroepithelial

¹Department of Mathematics, University of Hawaii, Honolulu, HI 96822, United States email: chyba@hawaii.edu, aaronts@hawaii.edu

² Department of Tropical Medicine, Medical Microbiology and Pharmacology, John. A. Burns School of Medicine, University of Hawaii, Honolulu, HI 96822, United States. email: fmercier@hawaii.edu

³ Graduate School of Mathematics, Kyushu University, Nishi-ku, Fukuoka, 819-0395, Japan email: zou@math.kyushu-u.ac.jp

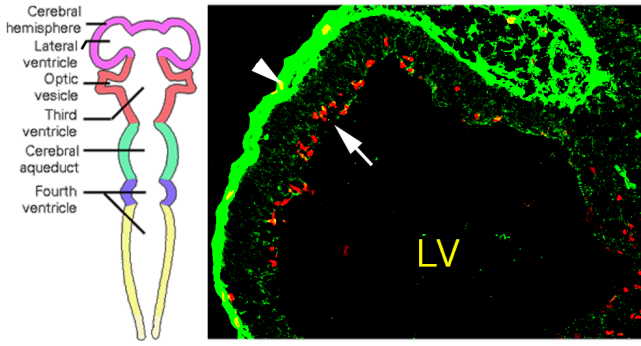


Fig. 1. Left: schematic representation of the formation of the lateral ventricles from the neural tube in vertebrate animals (dorsal view). Right: Brain section of a mouse embryo at the stage E10.5 (10.5 days of development) showing the development of the lateral ventricle (LV), a large cavity that derives from the neural tube (sagittal view). The arrowhead shows the meninges covering the developing brain. The arrow shows proliferating cells (immunolabeled for the mitotic marker phosphorylated-histone-3, red) and fractones (green puncta immunolabeled for the extracellular matrix marker laminin). As demonstrated by the green/red color associations, cells divide near fractones. This image was recorded with a Zeiss confocal laser scanning microscope, after indirect fluorescence immunohistochemistry. Experimental procedure: The brain section was first incubated with anti-phosphorylated-histone-3 and anti-laminin antibodies. Then, these primary antibodies were visualized by secondary antibodies conjugated to fluorophores AlexaFluor-546 (red) and AlexaFluor-488 (green) respectively.

cells, and neurogenic growth factors suggests that several steps of refinement will be necessary to expand the model and reach a satisfactory correlation between the mathematical simulations and the reality of controlled-cell proliferation in the developing brain. Similarly, on the biological side, experimental laboratory work is ongoing to provide data and support for the model.

II. THE MODEL

The ambient space in which the morphogenic events take place is identified to a fixed compact subset A of \mathbb{R}^2 . At this stage we do not want the ambient space to dictate the development of the cellular mass by preventing growth in any particular direction.

Definition The relevant components of morphogenesis under consideration are: the cells, the fractones, and the inter-cellular space in which growth factors diffuse. Due to the nature of morphogenic events, these spaces vary with time. They are precisely defined as follows:

- 1) The *cell space*, denoted $\text{Cell}(t)$, is a closed subset of A that represents the configuration of cells in the ambient space at a given time t .
- 2) The *diffusion space* at time t , denoted $\text{Diff}(t)$, is an open subset in A that represents the space in which growth factors diffuse. We have $\text{Diff}(t) = A \setminus \text{Cell}(t)$. At each time t , the diffusion space is split into two components: the free diffusion space, $\text{Free}(t)$, where the growth factors diffuse freely, and the fractone space, $\text{Fract}(t) = \text{Diff}(t) \setminus \text{Free}(t)$ where the diffusion is perturbed.

Fractones are extracellular structures key to our hypothesis. Viewed by transmission electron microscopy, fractones

appear as ‘fractal’ structures, that is to say highly-branched extracellular matrix structures [13]. However, with the lower resolution of confocal fluorescence microscopy, fractones are visualized as puncta [6], [9], [13] and figure 1. Our theoretical approach is based on the analysis of the distribution of fractones and their influence on cell proliferation throughout the neuroepithelium, and not on the relationships of one individual fractone with the few neighboring neuroepithelial cells. Therefore, our model will approach the morphogenic event at the scale of the neural tissue and will disregard the micro-scale fractal phenomena of a fractone. A fractone that triggers mitosis influences the deformation of the surrounding mass of cells depending on its location. More precisely, if the shape of the cell is identified to a circle, a fractone can be placed anywhere on the boundary of the circle. Once mitosis is induced by this fractone, the direction of the growth is determined by the position of the fractone on the circle. For our mathematical model, if ϵ represents the radius of the cell and $(0,0)$ its center, we distinguish between the four following positions for a fractone: $(\pm\epsilon, 0)$, $(0, \pm\epsilon)$. Those will be referred to as admissible fractone locations and will be denoted by $\text{Diff}_{\text{adm}}^{\text{frac}}(t)$. By definition $\text{Fract}(t)$ is the set of active fractones, therefore we have $\text{Fract}(t) \subset \text{Diff}_{\text{adm}}^{\text{frac}}(t)$. If an admissible fractone location does not contain an active fractone, then we say that it has a passive fractone.

A control system will be used to model the diffusion of the growth factors in $\text{Diff}(t)$. Notice that it is a perturbed diffusion due to our assumption that fractones capture and store the growth factors. Active fractones perturb the diffusion of the growth factors while the passive ones have no effects on the diffusion. In our system, the control represents the location of the active fractones, it will therefore take its value in the discretized set $\{0, 1\}$ since either a fractone is active or not. Since our experimental maps of fractone distribution only provides areas of high or low fractone concentrations rather than precise locations, we partition the space into regions and define a probability function on this partition for the existence of an active fractone in an admissible fractone location. In other words, we control the density of fractones in different regions of $\text{Diff}(t)$ as it evolves. To determine the probability that an active fractone is placed in a given admissible location at time t we introduce the following: Let $\mathcal{P}(t)$ be a partition of $\text{Diff}_{\text{adm}}^{\text{frac}}(t)$. Introduce $\text{Prob}_{\text{frac}}^t : \mathcal{P}(t) \rightarrow [0, 1]$, $P_i \mapsto \alpha_i$ where α_i is the probability that a fractone will become active at $P_i \in \mathcal{P}(t)$. Then to each $(a, b) \in P_i$ we use a random number generator to associate to (a, b) a number, $r_t(a, b) \in [0, 1]$. We define

$$u_t(a, b) = \begin{cases} 0 & \text{otherwise} \\ 1 & \text{if } r_t(a, b) < \alpha_i \end{cases} \quad (1)$$

In other words, the probability to have an active fractone in $(a, b) \in P_i$ is $\alpha_i * 100\%$.

The challenge is to find partitions and functions $\text{Prob}_{\text{frac}}^t$ that are plausible from a biological point of view. This needs to be guided by experimental observations.

A critical component of the biological system is the production and diffusion of the growth factors. We limit

ourselves in this first stage to one growth factor. For computational purposes, we start our simulations with a concentration of zero growth factor in $\text{Diff}(0)$ (this can easily be relaxed). We assume the production of growth factor to be a discrete process that happens at isolated times (this can easily be transformed into a continuous process). We set the production of growth factor to occur every multiple of a fixed parameter t_{prod} . More precisely, when $t = 0 \pmod{t_{prod}}$ growth factor is produced uniformly on the boundary of every cell by a quantity gf_{prod} set by the user. The diffusion of the growth factor then takes place as follows: In the absence of active fractones, diffusion is modeled by the classical heat equation. When an active fractone is present, however, we use a perturbed diffusion equation where the fractone acts as a point sink for the diffusion process: it stores growth factor, but appears to be empty with respect to our diffusion equation. This dynamical system will be described as an affine control system in section III once we introduce a discretization of the various spaces introduced earlier.

In addition to the evolution of the dynamical system, we must also take into account the fact that when the mother cell divides into two daughter cells, the existing mass of cells must deform to accommodate the new cells. The precise rules for deformation we use are described in the next section.

To summarize, we have the following: At the start of a simulation, fractones are placed in $\text{Diff}_{adm}^{frac}(t)$ according to a partition \mathcal{P} and values $\alpha_i, r_t(a, b)$. Until mitosis occurs, growth factor is produced, diffuses through the diffusion space, and is captured by the fractones. When a fractone reaches a prescribed threshold of captured growth factor, the corresponding cell undergoes mitosis. The mother cell divides into two daughter cells, and the existing cell space is adjusted according to our deformation algorithm. All fractones are then removed (any stored growth factor remains in place in the diffusion space) and reassigned according to the probability set by the user for the distribution of fractones (this probability can possibly change at each mitosis event).

III. COMPUTATIONAL ALGORITHM

We identify the ambient space A to its discretization which is now a subset of \mathbb{Z}^2 . The precision of the discretization is currently arbitrary, but will eventually be determined by experimental biological maps. To each point in A , which we will refer to as a unit, we assign an ordered pair of integers, (i, j) . The origin unit of our discretization is chosen arbitrarily and will be identified to $(0, 0)$. The distance between any two units is defined as the Euclidean distance between their assigned coordinates.

Biological cells are represented by 9×9 squares of units in the Cell space, with a 3 unit *channel* of diffusion space between neighboring cells. Fractones are a single unit in size. These choices are not completely arbitrary and are inspired by observations of brain tissue samples. Under this assumption, our admissible fractone locations are to the immediate left, right, top, or bottom of an existing cell, in-line with the center of the cell. For example, a cell centered at $(0, 0)$ could only have active fractones appear at $(5, 0)$,

$(-5, 0)$, $(0, 5)$, or $(0, -5)$. This means that each side of a cell will have at most one fractone associated with it. This assumption is somewhat restrictive, and will be relaxed in future work. We also define $\text{Cell}^*(t)$ as the set of all units $(a, b) \in \text{Cell}(t)$ that are the exact unit centers of existing cells at time t . We therefore have

$$\text{Diff}_{adm}^{frac}(t) = \bigcup_{\substack{(a,b) \in \text{Cell}^*(t) \\ (k,l) \in \Gamma}} \{(i, j) \in \text{Diff}(t); (i, j) = (a + k, b + l)\} \quad (2)$$

where $\Gamma = \{(5, 0), (-5, 0), (0, 5), (0, -5)\}$.

Initially, at time $t = 0$, no growth factor is present in any unit of the discretization of $\text{Diff}(0)$. Whenever the time is a multiple of the set production time, t_{prod} , growth factor is produced from every cell, as explained earlier. All units in $\text{Diff}(t)$ that are distance one from a unit in $\text{Cell}(t)$ have growth factor added to it by the amount gf_{prod} .

In the absence of a fractone, growth factors diffuse freely. In discrete terms, let $X_{i,j}(t)$ represent the amount of growth factor present in unit (i, j) at time t . For notational simplicity, we set $\Delta = \{(0, 1), (0, -1), (1, 0), (-1, 0)\}$. When $\text{Fract}(t)$ is empty, ie. no active fractone is present, we have at time t for $(i, j) \in \text{Diff}(t)$

$$\dot{X}_{i,j}(t) = \nu \sum_{\substack{(k, l) \in \Delta \\ (i+k, j+l) \in \text{Diff}(t)}} (X_{i+k, j+l}(t) - X_{i,j}(t)). \quad (3)$$

where ν is the diffusion coefficient.

Assume now that there is an active fractone in unit (i, j) , ie. $(i, j) \in \text{Fract}(t)$. We use a perturbed diffusion equation where the fractone acts as a sink. The perturbed diffusion for unit (i, j) and its three neighbors in the diffusion space (one of the four neighbors belongs to $\text{Cell}(t)$) becomes

$$\dot{X}_{i,j}(t) = \nu \sum_{\substack{(k, l) \in \Delta \\ (i+k, j+l) \in \text{Diff}(t)}} X_{i+k, j+l}(t) \quad (4)$$

$$\dot{X}_{i,j}(t) = \nu \sum_{\substack{(k, l) \in \Delta \\ (i+k, j+l) \in \text{Free}(t)}} (X_{i+k, j+l}(t) - X_{i,j}(t)) - \nu \cdot X_{i,j}(t) \quad (5)$$

where equation (4) represents perturbed diffusion for any (i, j) containing a fractone, and equation (5) represents perturbed diffusion for any unit $(i, j) \in \text{Diff}(t)$ that is an immediate neighbor of a fractone.

Both the free and the perturbed diffusions can be described by an affine control system as follows: At a given time t , the state space, $M(t)$, is defined as the concentration of growth factor in each unit that belongs to the diffusion space; that is, $M(t) = \mathbb{R}_{>0}^{dim(\text{Diff}(t))}$. We define the control $u(\cdot)$ to be a piece-wise constant function with values 1 or 0, $u : [0, T] \rightarrow \{0, 1\}$ where T is the duration of the morphogenic events under study. The control captures the information regarding the existence of an active fractone in a given unit of the diffusion space, the control in unit (i, j) is turned to 1 if there is an active fractone there otherwise its value is set to

0. We then have that the diffusion of the growth factor in $\text{Diff}(t)$ is governed by an affine control system [1], [2], [17], $X(t) \in M(t)$,

$$\dot{X} = F_0(X(t)) + \sum_{(i,j) \in \text{Diff}(t)} F^{(i,j)}(X(t))u_{(i,j)}(t) \quad (6)$$

where the drift F_0 represents the free diffusion (component (i, j) of this vector field is given by the right-hand side of equation (3)) and the control vector fields $F^{(i,j)}$ account for the effect of the perturbed diffusion when an active fractone exists in unit (i, j) (see the right-hand side of equations (4) and (5)).

The dynamic of the control function using the probabilistic approach explained in the previous section is then determined as follows. Given a partition $\mathcal{P} = \{P_1, \dots, P_n\}$ of $\text{Diff}_{\text{adm}}^{\text{frac}}(t)$, all units in P_s are assigned a number α_s , where $0 \leq \alpha_s \leq 1$. Then, using a random number generator we associate to every unit (k, l) in P_s a number $r_t^s(k, l)$. Component (k, l) of the control function $u(\cdot)$ takes value 1 if $r_t^s(k, l) \leq \alpha_s$ and 0 otherwise. The lower index t represents the fact that this procedure is time dependent. Setting $r_t^s(k, l)$ allows us to control the density of fractones in different regions of the diffusion space as the morphogenic events evolve. From a practical point of view, our current algorithm can reset the partition and the values $\alpha_s, r_t^s(k, l)$ immediately after mitosis occurs for one of the existing cells. Reallocating the densities of fractone distribution in the diffusion space is therefore a piecewise continuous process.

The final step of our algorithm deals with the deformation of the existing mass of cell when mitosis occurs. By our hypothesis, when a fractone captures sufficient growth factor, it triggers mitosis in its associated cell. When such an event happens, the mother cell will split into two daughter cells, potentially pushing neighbor cells. The location of the fractone in relation to its associated cell determines the direction of the push. By example, suppose there is a cell centered at $(0, 0)$ with a triggered fractone to its right at $(5, 0)$.

- 1) If the full 12×12 space to the right of the cell is in the free space, then the mother cell splits, leaving one the daughter cell centered at $(0, 0)$ and creating one cell centered at $(12, 0)$. Any associated fractones to the right, above, or below the mother cell transfer to the daughter cell centered at $(12, 0)$ while any associated fractones to the left of the mother cell remain with the daughter cell centered at $(0, 0)$.
- 2) If there is already an existing cell centered at $(12, 0)$, $(18, 0)$, $(18, 6)$, or $(18, -6)$ the division of the mother cell into two daughter cells deforms the existing mass of cells to the left and to the right. More precisely, the mother cell vanishes and the two daughter cells are created, centered at $(-6, 0)$ and $(6, 0)$. Associated fractones to the mother cell on the right, above, and below transfer to the daughter cell centered at $(6, 0)$. The other fractones transfer to the daughter cell centered at $(-6, 0)$. Existing cells that overlap these new cells undergo displacement (see below).

- 3) If there is already a cell centered at $(12, 6)$ or $(12, -6)$ (directly to the right of the mother cell, but half a cell above or below), the mother cell divides and fractones move as in (1). The cells at $(12, 6)$ and $(12, -6)$ undergo displacement (see below).

If mitosis is triggered by a fractone to the left, above, or below the associated cell the deformation of the existing mass of cells is done in an analogous fashion. The transfer of fractones to daughter cells is currently an arbitrary choice and may be changed in the future based on experimental observations.

Displacement of cells during a mitosis event is done according to the following algorithm:

- 1) If a cell is a direct neighbor to a new daughter cell deforming the existing mass (eg. $(0, 0)$ pushing into $(12, 0)$), then the cell is translated over 6 units in the direction of the deformation. All fractones transfer with it.
- 2) If a cell is an off-set neighbor to a new daughter cell deforming the existing mass, then the cell will be translated over 6 units perpendicular to the direction of the push. For instance, a mitosis event occurring on a mother cell centered at $(0, 0)$ deforming the existing mass to the right pushes a cell centered at $(12, 6)$ to be centered now at $(12, 12)$. All fractones transfer with it.

Note that one displacement of a cell may trigger another displacement, causing a chain reaction of displacements which generates the mass deformation. At the current stage, we do not take into account viscosity forces among cells. It is our goal to incorporate them into the model in forthcoming work. We also only allow growth in a horizontal or vertical direction. This is primarily due to the choice of square-shaped cell bodies in our discretization, and limits the flexibility for development of a cell mass.

Growth and displacement of cells additionally affect the distribution of growth factor. Indeed, during a mitosis event the dimension of $\text{Cell}(t)$ increases, which is equivalent to a decrease of the dimension of $\text{Diff}(t)$. Growth factor therefore needs to be redistributed in the new diffusion space. Due to a lack of space, we do not enter any technical details on the redistribution of the growth factor here. Roughly, 80% of any removed growth factor is evenly distributed one unit away from the boundary of the new cell space in the direction of the deformation and 20% is evenly distributed two units away. This create a wave of growth factor redistribution that moves with the growth of the mass of cells.

IV. SIMULATIONS

In this section we present simulations based on our computational algorithm. The first example represents two cellular growths from an identical initial mass configuration but associated to different probability distribution for the fractones' location. The second example demonstrates an approximation of post-neurulation events, in particular the initial stage of development of the lateral ventricle.

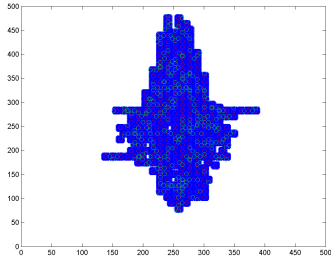
We initialize the calculations with $X_i(0) = 0$, ie. the concentration of growth factor in each unit of the diffusion

space is set to zero at the start of the simulation. The frequency of growth factor production by existing cells is set as $t_{prod} = 10$, and the amount of growth factor produced, $gf_{prod} = 10$. The threshold for captured growth factor to trigger mitosis, $gf_{thresh} = 100$. Diffusion constant, $\nu = .2$. As at this stage we are only testing the feasibility of the model, these parameters were chosen arbitrarily.

A. Random growth of cellular masses

For the first two simulations, we set the initial mass of cells to be four cells in a square configuration at the center of the ambient space. Each of the final masses of cells is obtained from a different partition of the admissible space for active fractones and probability for their existence.

Figure 2(b) represents the final mass of cells obtained from a trivial partition, $\mathcal{P} = \{\text{Diff}_{adm}^{frac}(t)\}$, and $\alpha_i = 0.25$. Therefore there is one chance out of 4 that a fractone becomes active at a location (a, b) of the admissible set for fractone placement. It can be observed that even though the distribution of fractones is set from a probabilistic point of view uniformly through the space a mass of cell gets elongated vertically. There are 308 mitosis events occurring between the initial mass of cells and the final one.



(a) Final mass of cell #1

Fig. 2. To obtain this final cellular mass we set a 25% probability of forming a fractone uniformly throughout the space.

Figure 3 is obtained from a nonuniform spatial probability for the distribution of fractones. More precisely, the simulation starts from the same 4 cells. The distribution probability is set to 80% for units $(i, j) \in \text{Diff}_{adm}^{frac}(t)$ that satisfies $i \geq 253, j \geq 253$, 25% for units $(i, j) \in \text{Diff}_{adm}^{frac}(t)$ that satisfies $i < 253, j \geq 253$, 16.67% for units $(i, j) \in \text{Diff}_{adm}^{frac}(t)$ that satisfies $i < 253, j < 253$ and 10% for all other units in $(i, j) \in \text{Diff}_{adm}^{frac}(t)$. This final mass was obtained after 335 mitosis events. Computationally it took 15 minutes to run the algorithm on a dual-core 2.4 GHz laptop with 64-bit operating system.

For both of the masses described above, we do not change the probability of the distribution of fractones during the entire period the morphogenic events took place. This will be explored in a forthcoming work with a corresponding analysis to determine a correlation between the probability and the cellular masses that we can create. In other words, the goal is to study how the control function affects the deformation of the mass of cells and develop control strategies to create desired shapes.

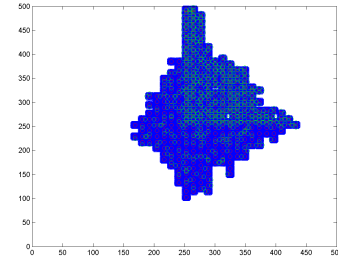


Fig. 3. Final mass of cell #2

B. Post-Neurulation and early formation of the lateral ventricles

To simulate an approximation of the formation of the lateral ventricles from the neural tube using our mathematical model we start with an initial ring of cells with an external vertical diameter of 100 cells (roughly 1200 units) and external horizontal diameter of 50 cells (roughly 600 units), and a thickness of five cells. See figure 4 (a).

The goal is to simulate the thickening of the walls of the neural tube and the development of “wing” structures on the left and right sides of the tube, and therefore to concentrate the density of fractones on the left and right edges of the ring. This produces the desired effect of expanding outward horizontally, but the interior cavity of the ring collapses slowly over time since our deformation algorithm tends to push cells both left and right, and does not create the shape we desire. On figure 4, the higher density of fractones on the far left and right of the ring shape has driven a greater degree of growth, thickening the two sides, while the top and bottom remain relatively thin, as desired. Further growth, however, does not produce the distinct wing-shapes we want. To produce better defined wing-shapes, the region of high density fractones on the edges was reduced to a narrower horizontal band, see figure 5. Within this band, and between the high density regions, fractones were not allowed, and near the interior of the ring, on the left and right sides, the density of fractones was increased slightly. However, this still did not produce the wing-shapes desired.

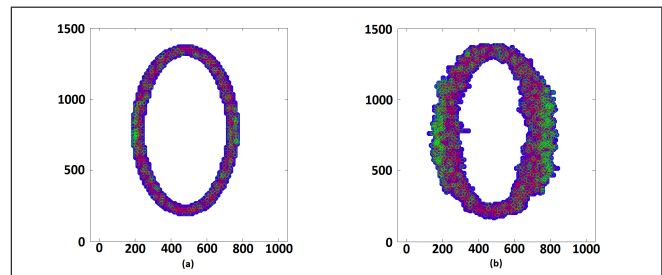


Fig. 4. (a) The initial configuration space when $t = 0$. (b) The mass of cells after 1225 mitosis events. Units $(i, j) \in \text{Diff}_{adm}^{frac}(t)$ such that $i < 211$ or $i > 751$ had a 25% probability to have an active fractone, while the other ones have a probability of 6.25%

Note that since we set the distribution probability for fractone placement at each mitosis event, we can exhibit

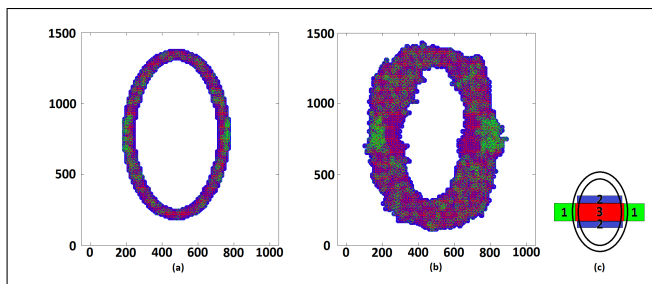


Fig. 5. (a) The initial configuration space when $t = 0$. (b) The mass of cells after 2451 mitosis events. (c) The partition and probability distribution. For $(i, j) \in \text{Diff}_{\text{adm}}^{\text{frac}}(t)$, when (i, j) is in one of the regions labelled 1, the probability of a fractone activating is 25%. When in a region labelled 2, the probability is 8.33%. When (i, j) is in a region labelled 3, the probability is set to zero. For all other (i, j) the probability is 6.24%.

a precise degree of control on how our cell space grows. We could, for example, set a zero probability at every $(i, j) \in \{\text{Diff}_{\text{adm}}^{\text{frac}}(t)\}$ except for one particular side of one particular cell, and thus guarantee that the cell will replicate in a particular direction. We could, therefore, produce a cellular mass very accurately to match the ideal target by carefully setting the partition and the $\alpha_s, r_t^s(k, l)$ values. However, because this assumes extremely precise knowledge of fractone placement over time during development, which we do not yet have, we choose to limit our precision to probabilities in general regions, setting higher probabilities in regions where more fractones are observed. As more experimental maps are available we will be able to refine our control strategy.

V. FUTURE WORK

There are several aspects of the biological process which are not yet incorporated into our current model. While we currently work exclusively in two-dimensions, our model is designed to easily extend to a more realistic three-dimensions. Diffusion, growth factor production, cell proliferation, and fractone placement are all readily translatable to a three-dimensional model. We will also consider situations with multiple growth factors (to capture inhibition) and more complex mechanisms for their production. Similarly, the condition that only one fractone is allowed per side of cell, and only at a prescribed location along each side, will be relaxed.

At present, our model cannot expand empty spaces, such as the interior cavity in the simulations above, since cells either grow into empty space or get pushed into the empty space. Thus in our simulations, the cavity always shrinks. In reality, the radius of the neural tube should be increasing, as observed in the lab. For this and the formation of the lateral ventricles from the primitive neural tube, it will be necessary to allow deformations of the cell mass by introducing a controlled *force*, separate from the pushing of mitosis, that causes cellular motion. Further considered additions for the model include cell migration and cell apoptosis (both of which are driven by growth factors).

One of our most important and interesting lines of study is how to systematically produce probability functions and

partitions to generate any desired cell mass. This is a complicated and rich problem that we will pursue moving forward.

ACKNOWLEDGMENT

This work was supported by the National Science Foundation Division of Graduate Education, award #0841223 and the National Science Foundation Division of Mathematical Sciences, award #1109937.

REFERENCES

- [1] B. Bonnard, M. Chyba "Singular Trajectories and their Role in Control Theory", Springer-Verlag, Series: Mathematics and Applications: Vol 40, 357 pgs, 2003.
- [2] A. Bressan, B. Piccoli "Introduction of Mathematical Theory of Control", Applied Math Series vol. 2, American Institute of Mathematical Sciences, 2007.
- [3] M. Chyba, M. Andonian, D. Cazzaro, L. Invernizzi, S. Grammatico "Modelling Cell-Fractone Dynamics Using Mathematical Control Theory". 50th IEEE Conf. on Decision and Control, Florida Dec. 2011.
- [4] M. Chyba, M. Kobayashi, F. Mercier, J. Rader, A. Tamura-Sato, G. Telleschi, Y. Kwon "A new Approach to Modeling Morphogenesis Using Control Theory", Special volume of the Sao Paulo Journal of Mathematical Sciences in honor of Prof. Waldyr Oliva, 2012.
- [5] M. Chyba, J. Mercier, J. Rader, Y. Kwon, R. Kodama "Dynamic Mathematical Modeling of Cell-Fractone Interactions", Journal of Math-For-Industry, Vol. 3, pp. 79-88, 2011.
- [6] V. Douet, E. Arikawa-Hirasawa, F. Mercier, Fractone-heparan sulfates mediate BMP-7 inhibition of cell proliferation in the adult subventricular zone, Neurosci. Let., vol. 528, pp.120-125, 2012.
- [7] J. E. Fata, Z. Werb, M.J. Bissell, Regulation of Mammary gland branching morphogenesis by the extracellular matrix and its remodeling enzymes, Breast Cancer Res. Vol. 6, pp.1-11, 2004.
- [8] Y. Furuta, D.W. Piston, B.L. Hogan, Bone morphogenetic proteins (BMPs) as regulators of dorsal forebrain development, Development, vol. 124, pp.2203-2212, 1997.
- [9] A. Kerever, J. Schnack, D. Vellinga, N. Ichikawa, C. Moon, E. Arikawa-Hirasawa, J. Efirid, F. Mercier, Novel extracellular matrix structures in the neural stem cell niche capture the neurogenic factor FGF-2 from the extracellular milieu, Stem Cells, vol. 25, pp. 2146-2157, 2007.
- [10] R. Levi-Montalcini, The nerve growth factor: its role in growth, differentiation and function of the sympathetic adrenergic neuron, Harvey Lect. Vol. 60, pp. 217-259. New York: academy press, 1966.
- [11] M. Martins, S. Warren, C. Kimberley, A. Marginanou, P. peschard, AMcCarthy, M. Yeo, C.J. Marshall, C. Dunsby, P.M.W. French, M. Katan, Activity of phospholipase C epsilon contributes to chemotaxis of fibroblasts towards platelet-derived growth factor, J. Cell Science, 2012, in press, epub. doi: 10.1242/jcs.110007
- [12] F. Mercier, E. Arikawa-Hirasawa, Heparan sulfate niche for cell proliferation in the adult brain, Neurosci. Let., vol. 510, pp. 7-72, 2012.
- [13] F. Mercier, J.T. Kitasako, G.I. Hatton, Anatomy of the brain neurogenic zones revisited: fractones and the fibroblast/macrophage network, J. Comp. Neurol., vol. 451, pp. 170-188, 2002.
- [14] F. Mercier, J. Schnack, M. Saint Georges-Chaumet, Fractones: home and conductors of the neural stem cell niche, In : Neurogenesis in the adult brain, Edit. A. Alvarez-Buylla, J.M. Parent, K. Sawamoto and T. Seki, vol. 1, Springer Verlag pub., 2011, pp. 109-136.
- [15] M. Murphy, K. Reid, M. Ford, J.B. Furness, P.F. Bartlett, FGF-2 regulates proliferation of neural crest cells, with subsequent neuronal differentiation regulated by LIF or related factors, Development, vol. 120, pp. 3519-3528, 1994.
- [16] J. Taipale, J. Keski-Oja, Growth factors in the extracellular matrix. FASEB J., 11:51-59 1997.
- [17] Eduardo D. Sontag "Mathematical Control Theory: Deterministic Finite Dimensional Systems", Second Edition, Springer, New York, 1998. (531+xvi pages, ISBN 0-387-984895)